

## Molecular solids of actinide hexacyanoferrate: Structure and bonding

This content has been downloaded from IOPscience. Please scroll down to see the full text.

2010 IOP Conf. Ser.: Mater. Sci. Eng. 9 012026

(<http://iopscience.iop.org/1757-899X/9/1/012026>)

View [the table of contents for this issue](#), or go to the [journal homepage](#) for more

### Download details:

IP Address: 150.214.182.116

This content was downloaded on 30/09/2016 at 14:53

Please note that [terms and conditions apply](#).

You may also be interested in:

[State-of-the-art coordination chemistry of radioactive elements](#)

B I Kharisov and Miguel A Mendez-Rojas

[The Quantum Chemistry of Unusual Oxidation States of the Lanthanides and Actinides](#)

V I Spitsyn and Galina V Ionova

[Low-dimensional systems investigated by x-ray absorption spectroscopy: a selection of 2D, 1D and 0D cases](#)

Lorenzo Mino, Giovanni Agostini, Elisa Borfecchia et al.

[Recent advances in x-ray absorption spectroscopy](#)

Heiko Wende

[Some Aspects of the Coordination Chemistry of the Lanthanides](#)

Victor T Panyushkin, Yu A Afanas'ev, Alexander D Garnovskii et al.

[Complex phosphates formed by metal cations in oxidation states I and IV](#)

Vladimir I Pet'kov

[Electron paramagnetic resonance from actinide elements](#)

L A Boatner and M M Abraham

## Molecular solids of actinide hexacyanoferrate: Structure and bonding

G Dupouy<sup>1</sup>, T Dumas<sup>1</sup>, C Fillaux<sup>1</sup>, D Guillaumont<sup>1</sup>, P Moisy<sup>1</sup>, C Den Auwer<sup>1\*</sup>, C Le Naour<sup>2</sup>, E Simoni<sup>2</sup>, E G. Fuster<sup>3</sup>, R Papalardo<sup>3</sup>, E Sanchez Marcos<sup>3</sup>, C Hennig<sup>4</sup>, A Scheinost<sup>4</sup>, S D Conradson<sup>5</sup>, D K. Shuh<sup>6</sup> and T Tyliszczak<sup>6</sup>

<sup>1</sup> CEA, Nuclear Energy Division, Radiochemistry Process Department, SCPS, LILA, 30207 Bagnols sur Cèze, France

<sup>2</sup> IPN, Paris XI University, 91405 Orsay, France

<sup>3</sup> University of Sevilla, Physical Chemistry Department, 41012 Sevilla, Spain

<sup>4</sup> Forschungszentrum Dresden-Rossendorf, 01314 Dresden, Germany

<sup>5</sup> Los Alamos National Laboratory, Los Alamos, NM87545, USA

<sup>6</sup> Lawrence Berkeley National Laboratory, Berkeley, CA 94720, USA

E-mail: christophe.denauwer@cea.fr

**Abstract.** The hexacyanometallate family is well known in transition metal chemistry because the remarkable electronic delocalization along the metal-cyano-metal bond can be tuned in order to design systems that undergo a reversible and controlled change of their physical properties. We have been working for few years on the description of the molecular and electronic structure of materials formed with  $[\text{Fe}(\text{CN})_6]^{n-}$  building blocks and actinide ions ( $\text{An} = \text{Th}, \text{U}, \text{Np}, \text{Pu}, \text{Am}$ ) and have compared these new materials to those obtained with lanthanide cations at oxidation state +III. In order to evaluate the influence of the actinide coordination polyhedron on the three-dimensional molecular structure, both atomic number and formal oxidation state have been varied : oxidation states +III, +IV. EXAFS at both iron K edge and actinide  $L_{\text{III}}$  edge is the dedicated structural probe to obtain structural information on these systems. Data at both edges have been combined to obtain a three-dimensional model. In addition, qualitative electronic information has been gathered with two spectroscopic tools : UV-Near IR spectrophotometry and low energy XANES data that can probe each atom of the structural unit : Fe, C, N and An. Coupling these spectroscopic tools to theoretical calculations will lead in the future to a better description of bonding in these molecular solids. Of primary interest is the actinide cation ability to form ionic – covalent bonding as 5f orbitals are being filled by modification of oxidation state and/or atomic number.

### 1. Introduction

The hexacyanometallate family is well known in transition metal chemistry because the remarkable electronic delocalization along the metal–cyano–metal bond can be tuned in order to design systems that undergo a reversible and controlled change of their physical properties. Evidence of photomagnetic effects

in Prussian Blue analogues was a critical step in this domain and showed that molecular excitation can induce long-range magnetic order. For example, the well known face-centered cubic structure of Prussian Blue derivatives form alternating M and M' ions chains that are linked by cyanide bridges [1]. In a more general way, the properties of the cyano bond makes it a very interesting candidate for fundamental investigation of electronic delocalization involving cations with delocalized or partially delocalized valence electrons (e.g., as 3d electrons). The recent publication of Hocking *et al.* underlines the particularity of the iron-cyano bond in ferri and ferrocyanide [2]. Several other studies have also been devoted to the structural and electronic characterization of the Prussian Blue derivatives [3].

The hexacyanometallate derivatives of f elements have also been reported, although to a much smaller extent and mainly for lanthanide derivatives. From a fundamental aspect, the molecular chemistry of actinides is a challenging issue for physical chemists because the understanding of the properties of heavy cations is still hampered by the large number of electrons. In comparison with transition metal in the one hand and lanthanide elements in the other hand, early actinides may be viewed as intermediates (although this is simplistic) in the sense that their valence 5f orbitals may be partially available for chemical bonding, in contrast with lanthanide elements that mainly form pure ionic bonds. The "5f" orbital extension is therefore considered rather large compared to the "4f" extension. From a more utilitarian perspective, potential applications in the frame of the minor actinide – lanthanide separation lead to preliminary results of selective precipitation [4]. In addition, nitrogen donor ligands have always been of interest as potential candidates for ionic recognition purposes (selective separation processes, sequestering agents, etc.). Fuel reprocessing from nuclear power plants, repository risk assessment and potential toxicological impact of spent nuclear fuel are some of the major issues of the countries using nuclear power to protect their population and to propose a competitive and sustainable energetic mix for the 21st century. For example, fuel reprocessing based on hydrometallurgical techniques is at the motivation behind both fundamental and applied research work in liquid-liquid extraction aiming to improve the design of extracting molecules. Hexacyanoferrate  $[\text{Fe}(\text{CN})_6]^{n-}$  anions coordinated to actinide ions were first mentioned during the 1950's [5] with plutonium. A variety of  $\text{M}_x(\text{UO}_2)_y[\text{Fe}(\text{CN})_6]_z \cdot w\text{H}_2\text{O}$  compounds were synthesized and used as sorbants [6] but only the uranyl adduct of these [actinide/ $\text{Fe}(\text{CN})_6$ ] complexes was structurally characterized [7]. Only the X-ray Powder Diffraction of the complex  $\text{Th}^{\text{IV}}[\text{Fe}^{\text{II}}(\text{CN})_6] \cdot 5\text{H}_2\text{O}$  had been reported [8] showing that it crystallizes in the same hexagonal space group as  $\text{Ln}^{\text{III}}\text{K}[\text{Fe}^{\text{II}}(\text{CN})_6] \cdot 4\text{H}_2\text{O}$  (Ln=La – Nd) does. A few years ago we have started describing the molecular and electronic structure of the materials formed by  $[\text{Fe}(\text{CN})_6]^{n-}$  building blocks and actinide ions (Th, U, Np) [9]. We have compared these new materials to the analogues obtained with lanthanide cations. Our major interest was to describe the distinct nature of the An–NC–Fe (An = actinide cation) bonding and the structural consequences of incorporating rigid building blocks in the actinide coordination sphere. Preliminary spectrophotometric measurements on the Np(IV) adducts have suggested that a partial electronic delocalization might occur along the cyano bond. It was also found from combined X-ray Absorption Spectroscopy (XAS) and X-ray diffraction studies that both actinide and lanthanide compounds were isostructural (hexagonal) in contrast with the cubic phases usually observed for transition metals [10]. In these cases, the EXAFS data indicate that the hexacyanoferrate molecular entity is conserved and the lanthanide or actinide cation is incorporated in the structure through nitrogen bonding of the cyano ligands. The remainder of the cation coordination sphere is then filled with water molecules. Note that actinide chemistry is complicated by a versatile redox chemistry compared to the lanthanides. Evidence for a competition between the actinide redox potential and the crystal field has been assumed in order to explain the occurrence of Np(IV) instead of Np(III) in the case of Np hexacyanoferrate. To date, the mechanisms that underlie the formation of these three-dimensional structures are still a matter of debate, especially in terms of electronic properties. Additional difficulty comes from the fact that fundamental understanding of actinide physical-chemistry is still at the early stages compared to d-

transition metals. In this family, the 5f and 6d frontier orbitals are engaged in the chemical bonding and their properties reflect the nature of the actinide–ligand bonding.

## 2. Experimental

Details about sample preparation and description of the EXAFS data fitting procedure will be given in a coming article [11]. Details about the study of aqueous californium cation by a combination of EXAFS data and theoretical calculations will also be provided in a future article [12].

### 2.1. Synthesis

Hexacyanoferrate compounds were prepared in aqueous acidic solutions by adding the actinide solution into the hexacyanoferrate solution. All the hexacyanometallates compounds were obtained by direct precipitation from the aqueous solution. After centrifugation and removal of the solution, precipitate was rinsed two times with ethanol and dried one time with acetone.

Three compounds are described in this paper : Am(III)/[Fe(II)(CN)<sub>6</sub>] (denoted **Am<sup>III</sup>/Fe<sup>II</sup>** in the following), Cf(III)/[Fe(II)(CN)<sub>6</sub>] (noted **Cf<sup>III</sup>/Fe<sup>II</sup>**), Th(IV)/[Fe(II)(CN)<sub>6</sub>] (denoted **Th<sup>IV</sup>/Fe<sup>II</sup>**) and Np(IV)/[Fe(II)(CN)<sub>6</sub>] (denoted **Np<sup>IV</sup>/Fe<sup>II</sup>**). In the An(III)/[Fe(II)(CN)<sub>6</sub>] compounds, charge compensation most probably occurs with K as in the lanthanide case. The <sup>241</sup>Am(III) solution was prepared by dissolution of AmO<sub>2</sub> (CEA stock) in nitric acid. The <sup>249</sup>Cf(III) solution was purified from an ill-defined old solution of <sup>249</sup>Cf (~100 MBq) from IPN Orsay with a strong radiation damage of the first container. Part of the solution was evaporated to dryness and the voluminous foamy residue was taken up in concentrated HCl. The cloudy solution was centrifuged and the supernatant percolated on a column filled with an anion exchanger (Bio-Rad AG-MP 1, 100-200 mesh). Then the eluted fractions were evaporated to dryness and taken up in dilute HCl. The so obtained solution was percolated through a column filled with a cation exchanger (Bio-Rad AG-MP 50, 100-200 mesh). The purified fractions were gathered and evaporated to dryness. No deposit was visible to the naked eye. The container was then rinsed with HClO<sub>4</sub> to obtain the stock californium solution. This stock solution was used to prepare the aquo **Cf<sup>3+</sup>** sample. The <sup>232</sup>Th(IV) solution was obtained by dissolving Th(NO<sub>3</sub>)<sub>4</sub>.5H<sub>2</sub>O (prolabo) in nitric acid. Finally the stock solution of <sup>237</sup>Np(IV) was prepared by hydroxylammonium chloride reduction (70 °C) of a Np(V) solution previously obtained by dissolution of Np(V)O<sub>2</sub>OH·xH<sub>2</sub>O (x ≈ 2.5) in hydrochloric acid. The reaction was monitored by spectrophotometry in order to control neptunium concentration, and to insure that less than 1% Np(V) remained in the solution.

### 2.2. XAS data acquisition

EXAFS spectra were recorded at the European Synchrotron Radiation Facility (ESRF) (6 GeV at 200 mA) and at the Stanford Synchrotron Radiation Laboratory (SSRL) (3 GeV at 100 mA).

Californium, thorium and neptunium L<sub>3</sub> edge EXAFS spectra were recorded at the Rossendorf beam line of the ESRF (BM20). BM20 is equipped with a water cooled double crystal Si(111) monochromator. Higher harmonics were rejected by two collimating Pt coated mirrors. A 13-element Ge solid state detector was used for data collection in the fluorescence mode.

Americium L<sub>3</sub> edge EXAFS spectra were recorded on beam line 11-2 of SSRL. The beam line is equipped with a liquid nitrogen cooled double crystal Si(220) monochromator, and with two collimating and focusing rhodium coated mirrors. A 30-element Ge solid state detector was used for data collection in the fluorescence mode.

Monochromator energy calibration for the actinide absorption spectra was carried out at yttrium or zirconium K-edge. All measurements were recorded in double layered cells of 200 μL specifically designed for radioactive samples, at room temperature.

Iron  $L_{2,3}$  edges were recorded at the 11.0.2 beamline of the Advanced Light Source (ALS, Lawrence Berkeley National Laboratory, U.S.A), particularly relevant for radioactive materials and soft X-ray experiments in the STXM mode.

### 2.3. XAS data processing

Data were processed using the Athena code [13]. Background removal was performed using a pre-edge linear function. Atomic absorption was simulated with a cubic spline function. The extracted EXAFS signal was fitted in R space without any additional filtering using the ARTEMIS code. The pseudo-radial distribution functions (PRDF) are given by the Fourier transform calculated in  $k^3\chi(k)$  and  $k^2\chi(k)$  for aqueous  $Cf^{3+}$ .

Phases and amplitudes were calculated with Feff82 code [14] based on the crystal structure of  $[Lu(DMF)_4(H_2O)_3(Fe^{III}(CN)_6)] \cdot H_2O$  which has been synthesized as a monocrystalline compound identical to that reported in the literature [15]. For aqueous  $Cf^{3+}$ , phases and amplitudes were calculated from theoretical model [12].

## 3. Results and discussion

### 3.1. EXAFS data at the americium and californium edges.

The isomorphous series of  $LnKFe(CN)_6 \cdot 4H_2O$  ( $Ln = La, Nd$ ) compounds has been described in the late eighties in the hexagonal space group [16]. Since then, several occurrences have been reported with various stoichiometries and structures depending largely on atomic number of the lanthanide cation. Within this series, actinide(III) have never been described although they are expected to behave similarly as their lanthanide analogues. We have decided to investigate the middle of the actinide series with typical actinide(III) candidates : Am and Cf.

The EXAFS spectra of  $Am^{III}/Fe^{II}$  and  $Cf^{III}/Fe^{II}$  at the americium and californium  $L_3$  edge have been recorded and experimental spectra are reported in Figure 1.

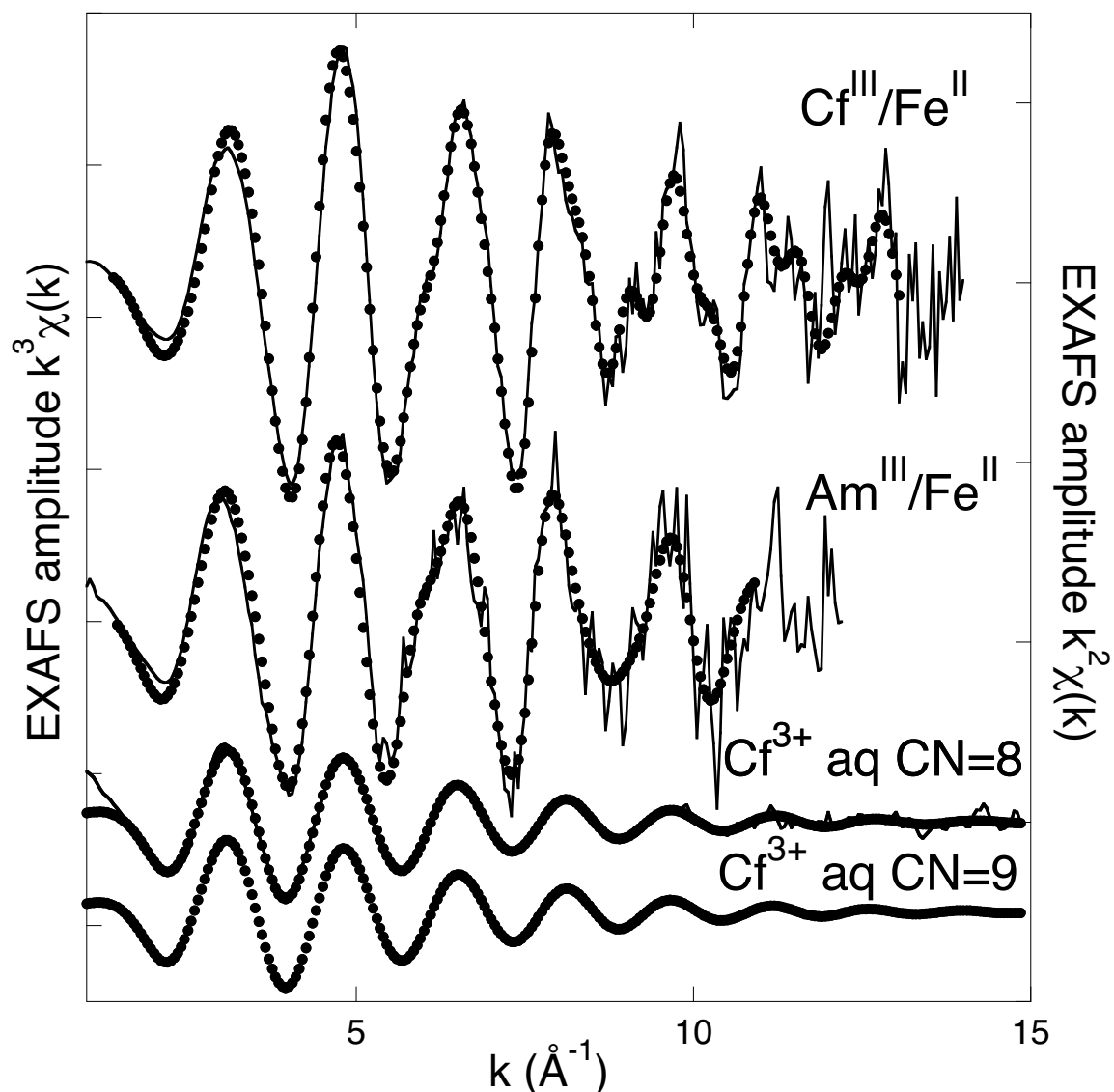


Fig. 1 : Experimental (straight line) and fitted (dots) EXAFS spectra at the actinide  $L_3$  edge of  $\text{Am}^{\text{III}}/\text{Fe}^{\text{II}}$  and  $\text{Cf}^{\text{III}}/\text{Fe}^{\text{II}}$  hexacyanometallate compounds (left scale) and of aquo  $\text{Cf}^{\text{3+}}$  ion in perchloric acid solution (right scale). CN=8 means that fitting has been performed with a Square Antiprism configuration, CN=9 means that fitting has been performed with a Trigonal Tricapped Prism configuration.

The two spectra of the cyanometallate compounds have been fitted with four different shells according to our previous results [10] : a first shell of nitrogen atoms from the cyano ligand, a second shell of oxygen atoms from water molecules, a third shell of carbon atoms from the cyano ligand and a fourth shell of iron from the hexacyanoferrate unit. Table 1 summarizes the best parameters obtained from the EXAFS data fitting. The obtaining of a satisfactory fit using this fitting procedure confirms that all compounds exhibit a cyano-bridge structure in which the hexacyanoferrate anion may be viewed as a semi-rigid molecular brick. In a near future, the iron K edge of all the compounds will also be recorded, allowing to fit both edges in the same time with a set of linked geometric parameters.

A this point of the study, the actinide(III) environment may be compared to that of lanthanides in the corresponding hexacyanoferrate(II) series. For instance KNd(III)Fe(II)CN<sub>6</sub>.4H<sub>2</sub>O crystallizes in the P63/m space group (hexagonal) [17], the neodymium cation being at the centered of a trigonal tricapped prism (6+3) formed by the 6 nitrogen atoms of the cyano ligand and 3 additional water molecules at the capping position : Nd-N = 2.518 Å, Nd-O = 2.685, Nd-Fe = 5.47 Å. KGd(III)Fe(II)CN<sub>6</sub>.3.5H<sub>2</sub>O crystallizes in the Cmc<sub>2</sub>m space group (orthorhombic) and KGd(III)Fe(II)CN<sub>6</sub>.3H<sub>2</sub>O crystallizes in the Pnma space group (orthorhombic). In KGd(III)Fe(II)CN<sub>6</sub>. 3.5H<sub>2</sub>O, the gadolinium cation sits in a tricapped trigonal prism (CN = 6+3, Gd-N = 2.37 Å, Gd-O = 2.48 Å, Gd-Fe = 5.41 Å) while the coordination sphere of KGd(III)Fe(II)CN<sub>6</sub>. 3H<sub>2</sub>O is best described as a bicapped trigonal prism (Pnma : 6+2, Gd-N = 2.43 Å, Gd-O = 2.57 Å, Gd-Fe = 5.40 Å). A direct comparison between the distances obtained by EXAFS with **Am<sup>III</sup>/Fe<sup>II</sup>** and **Cf<sup>III</sup>/Fe<sup>II</sup>** and the above distances reported in the literature suggests that on the one hand the americium and neodymium environment are very similar (P63/m space group) and on the other hand the californium and gadolinium environment are very similar (Pnma space group). Within this picture the actinide coordination number is 9 in **Am<sup>III</sup>/Fe<sup>II</sup>** and 8 in **Cf<sup>III</sup>/Fe<sup>II</sup>**. This suggests a decrease of the coordination number from americium to californium from trigonal tricapped prism to trigonal bicapped prism. X-ray powder diffraction measurements are currently being undertaken in order to confirm this analogy between the space groups of the lanthanide and actinide compounds. This will also allow, together with the EXAFS parameterized fits to derive the An-NC bond angle and compare it with the lanthanide analogues.

Table 1 : EXAFS best fit parameters of **Am<sup>III</sup>/Fe<sup>II</sup>**, **Cf<sup>III</sup>/Fe<sup>II</sup>** solid compounds and aquo **Cf<sup>3+</sup>** ion.

compound	An-N, An-O, Å	An-C (linked), Å	An-Fe (linked), Å
<b>Am<sup>III</sup>/Fe<sup>II</sup></b>	6 N at 2.49(2), $\sigma^2 = 0.0065 \text{ \AA}^2$ 3 O at 2.69(2), $\sigma^2 = 0.0108 \text{ \AA}^2$	3.52, $\sigma^2 = 0.0017 \text{ \AA}^2$	5.33, $\sigma^2 = 0.0218 \text{ \AA}^2$
<b>Cf<sup>III</sup>/Fe<sup>II</sup></b>	6 N at 2.44(2), $\sigma^2 = 0.0068 \text{ \AA}^2$ 2 O at 2.57(2), $\sigma^2 = 0.0121 \text{ \AA}^2$	3.51, $\sigma^2 = 0.0094 \text{ \AA}^2$	5.35, $\sigma^2 = 0.0050 \text{ \AA}^2$
<b>aquo Cf<sup>3+</sup>(1)</b>	8 O at 2.42(1) $\sigma^2 = 0.0082 \text{ \AA}^2$		
<b>aquo Cf<sup>3+</sup>(2)</b>	6 O at 2.38(1) $\sigma^2 = 0.0068 \text{ \AA}^2$ 3 O at 2.47(1) $\sigma^2 = 0.0039 \text{ \AA}^2$		

**Am<sup>III</sup>/Fe<sup>II</sup>**  $e_0 = 6.8 \text{ eV}$ ,  $S_0^2 = 1.1$ ,  $r = 4.0\%$ , **Cf<sup>III</sup>/Fe<sup>II</sup>**  $e_0 = 4.9 \text{ eV}$ ,  $S_0^2 = 1.1$ ,  $r = 4.0\%$ , **aquo Cf<sup>3+</sup>(1)**  $e_0 = 1.8 \text{ eV}$ ,  $S_0^2 = 1.0$ ,  $r = 1.8\%$ , **aquo Cf<sup>3+</sup>(2)**  $e_0 = 1.8 \text{ eV}$ ,  $S_0^2 = 0.9$ ,  $r = 1.9\%$

In order to better understand the structural break that has been observed in the An<sup>III</sup>/Fe<sup>II</sup> hexacyanometallate family between americium and californium, we have also undertaken the study of Cf<sup>3+</sup> in acidic perchloric solution. Although this question will be subject of a detailed article in the near future [12], we would like to report here our preliminary results. Figure 1 shows the experimental EXAFS spectrum of the aquo californium cation. It is well known that the Ln<sup>3+</sup> and An<sup>3+</sup> cations in aqueous solution occur with different polyhedra (typically 6+3, 6+2 or 8 coordination numbers) depending largely on their ionic size. This question has been a matter of debate in the literature [18,19] and discussed in full details by Skanthakumar *et al.* for the aqueous curium cation [20]. In the solid state, comparison can be found with curium and americium [21] in the hydrated adducts. It is beyond the scope of this report to discuss this question in the same details for californium. In a previous article, we have provided a first estimate of the Cf-O<sub>aq</sub> distance with no *a priori* restriction on the coordination polyhedron [22]. Once again, we have recorded the data lately, with an extended k range. It has been fitted according to two typical distinct models : square antiprism (SA, CN = 8) and tricapped trigonal prism (TTP, CN = 6+3). Figure 1 and Table 1 show the output of the two adjustments with no clear distinction between the two

results : 8 oxygen atoms at 2.42 Å for SA, 9 oxygen atoms at 2.41 Å for the weighted average of TTP, keeping in mind that a difference of one unit in coordination number over i.e. 9 (11%) is not significant from the EXAFS point of view, especially in the absence of experimental  $S_0^2$  value. These values are in very good agreement with our former result : 8.5 O at 2.42 Å. In comparison, the Am-O<sub>aq</sub> distance has been reported to be 10.3 O at 2.48 Å [23] in HCl solution. The decrease of 0.06 Å between the aquo forms of Am<sup>3+</sup> and Cf<sup>3+</sup> is comparable to that of 0.05 Å for the nitrogen coordination sphere of the hexacyanometallates described above, although a direct comparison is not rigorous because of the possible changes in coordination numbers that are not discussed here.

We may assume from these data that californium represents a step in the description of coordination polyhedra, in comparison with gadolinium in the hexacyanometallate series. In aqueous solution, a more detailed investigation combined with molecular dynamics simulations will be provided in the near future [12].

### 3.2. Investigation of the actinide cyano bond in $\text{Th}^{\text{IV}}/\text{Fe}^{\text{II}}$ and $\text{Np}^{\text{IV}}/\text{Fe}^{\text{II}}$

It is well known that Prussian Blue analogues exhibit various colors, Prussian Blue,  $\text{Fe}^{\text{III}}_4[\text{Fe}^{\text{II}}(\text{CN})_6]_3 \cdot 14\text{H}_2\text{O}$ , itself occurring as a well known deep blue compound. In the case of the actinide analogues described here, strong discrepancies in colors have also been observed :  $\text{Th}^{\text{IV}}/\text{Fe}^{\text{II}}$  is white and turns pale blue with time because of growing contamination with Prussian Blue;  $\text{Np}^{\text{IV}}/\text{Fe}^{\text{II}}$  is deep red-pink,  $\text{Am}^{\text{III}}/\text{Fe}^{\text{II}}$  is pale pink and  $\text{Cf}^{\text{III}}/\text{Fe}^{\text{II}}$  is white. This macroscopic observation already suggests some specific behavior of each actinide element at a given oxidation state towards hexacyanoferrate bonding.

Figure 2 shows the spectrophotometric absorption spectra measured in total reflection mode of  $\text{Th}^{\text{IV}}/\text{Fe}^{\text{II}}$  and  $\text{Np}^{\text{IV}}/\text{Fe}^{\text{II}}$  compared to that of Prussian Blue. Because of its deep blue color, Prussian Blue exhibits a strong absorption band around 730 nm.  $\text{Np}^{\text{IV}}/\text{Fe}^{\text{II}}$  exhibits a similar band around 460 nm. The corresponding absorption spectrum measured in transmission mode on a KBr pellet clearly exhibits the two peaks characteristic of Np(IV) cation, but shifted in energy with respect to the free aquo ion : 982 nm (aquo = 960 nm) and 697 – 755 nm (aquo = 723 nm).  $\text{Th}^{\text{IV}}/\text{Fe}^{\text{II}}$  does not exhibit any strong absorption band, in agreement with its white color.



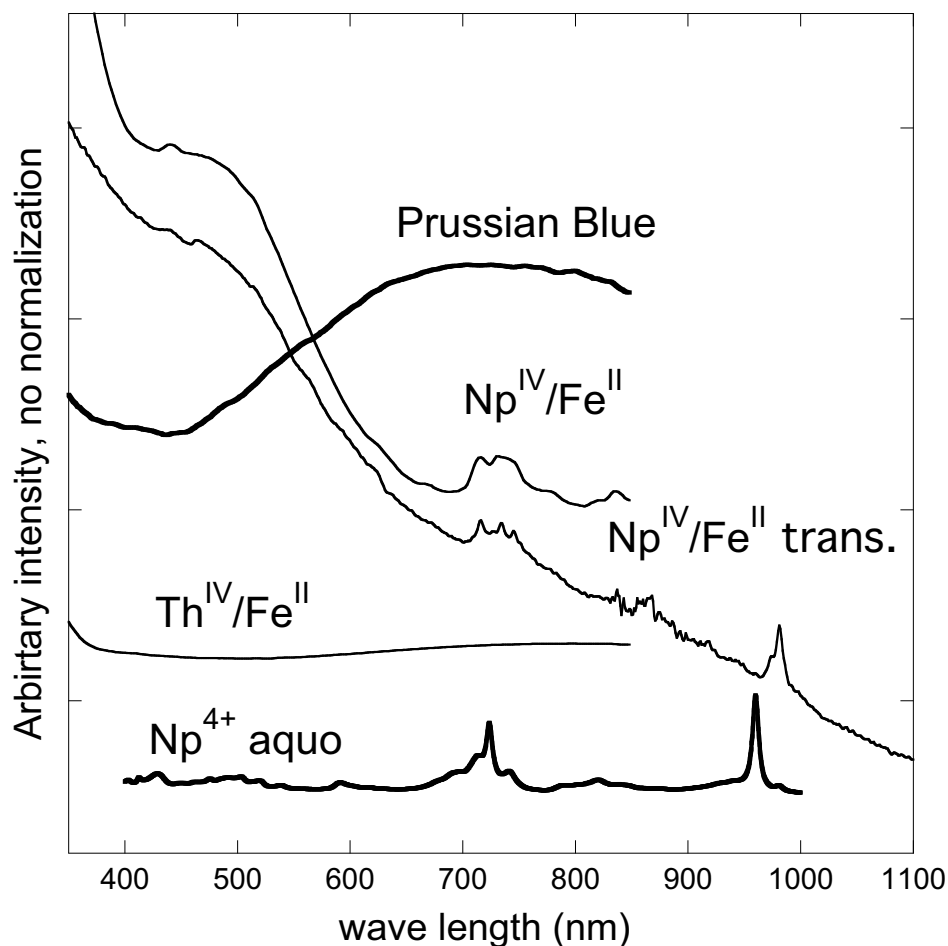


Fig. 2 : Spectrophotometric absorption spectra of Prussian Blue,  $\text{Th}^{\text{IV}}/\text{Fe}^{\text{II}}$  and  $\text{Np}^{\text{IV}}/\text{Fe}^{\text{II}}$  in total reflection mode and in transmission mode ( $\text{Np}^{\text{IV}}/\text{Fe}^{\text{II}}$  trans.). Comparison with aqueous  $\text{Np}^{4+}$  cation in acidic solution.

In order to better understand the role of the 5f electrons in the actinide-cyano bonding within this family of molecular solids, we have recently undertaken a systematic study of the X-ray Absorption edges of all the atoms of the compound : Fe  $L_{2,3}$  edges, C and N K edge and An  $N_{4,5}$  and  $M_{4,5}$  edges. This should provide a clear picture of the An-NC-Fe bonding mode and its evolution across the actinide series by probing directly the Fe 3d orbitals, ligand antibonding molecular orbitals (2p character) and actinide 5f orbitals. Although this work is at the starting point we provide here a qualitative comparison between the iron  $L_{2,3}$  edges in  $[\text{Fe}(\text{II})(\text{CN})_6]^{4-}$ ,  $[\text{Fe}(\text{III})(\text{CN})_6]^{3-}$  and in  $\text{Th}^{\text{IV}}/\text{Fe}^{\text{II}}$  and  $\text{Np}^{\text{IV}}/\text{Fe}^{\text{II}}$ . The spectra are compared in Figure 3.

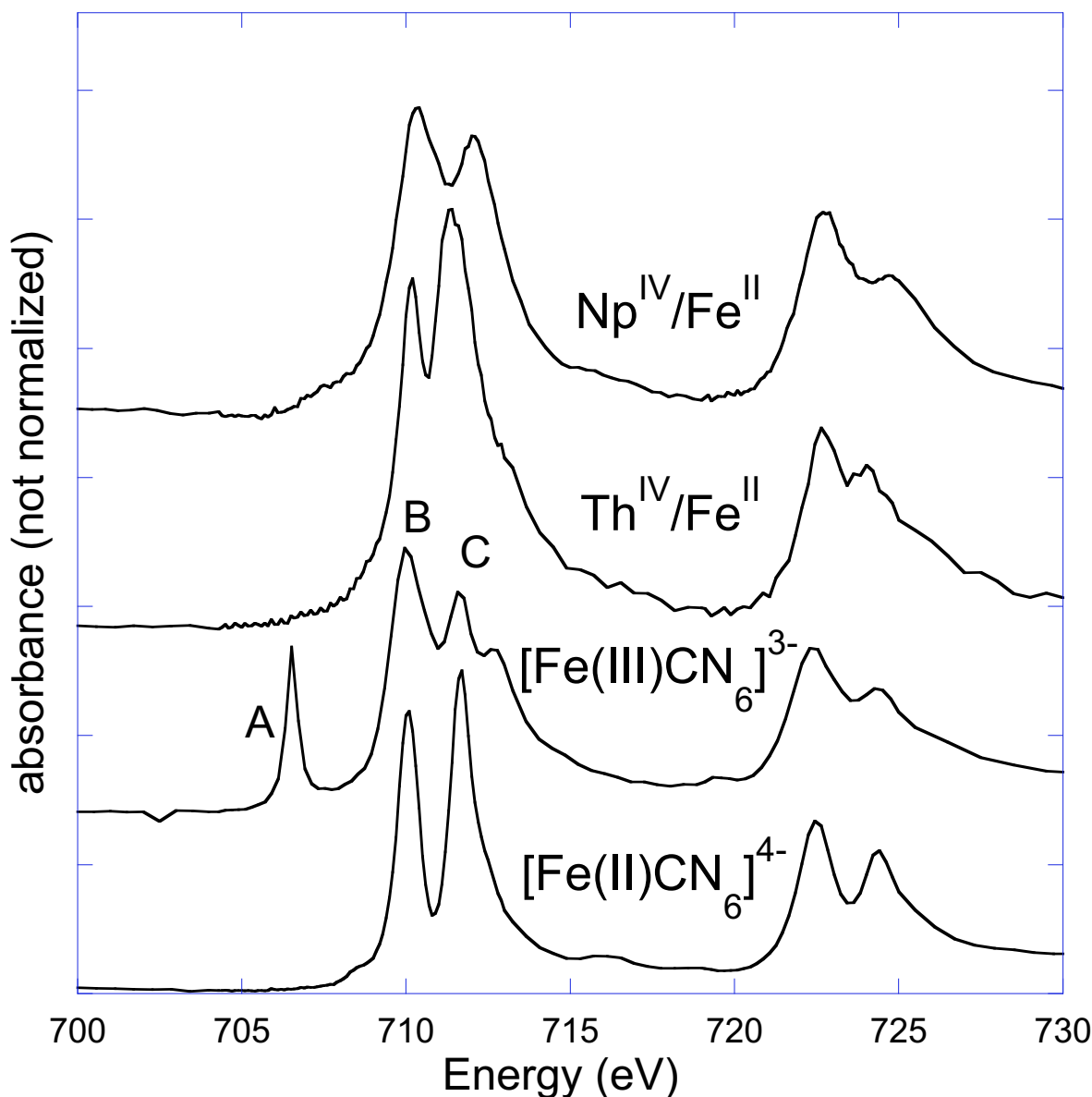


Fig.3 : Iron  $L_{2,3}$  edges of  $[\text{Fe}(\text{II})(\text{CN})_6]^{4-}$ ,  $[\text{Fe}(\text{III})(\text{CN})_6]^{3-}$ ,  $\text{Th}^{\text{IV}}/\text{Fe}^{\text{II}}$  and  $\text{Np}^{\text{IV}}/\text{Fe}^{\text{II}}$ .

The iron  $L_{2,3}$  edges of  $[\text{Fe}(\text{II})(\text{CN})_6]^{4-}$  and  $[\text{Fe}(\text{III})(\text{CN})_6]^{3-}$  have extensively been described by Hocking and co-authors [24]. Peak A in  $[\text{Fe}(\text{III})(\text{CN})_6]^{3-}$  corresponds to a low energy transition to the empty hole in the  $t_{2g}$  orbital of iron. Peaks B and C have been assigned first to a transition to the  $e_g^*$  orbital and second to the  $t_{2g}^*/\pi^*$  orbital originating from the metal to ligand backbonding ability of the cyano-iron bond. Therefore the ratio intensity between peak B and C seems to be related to the charge transfer : back-donation from iron to the cyano antibonding orbital. In Figure 3, the spectrum of  $\text{Th}^{\text{IV}}/\text{Fe}^{\text{II}}$  is very distinct from that of the other actinide hexacyanometallates. But it compares with the spectrum of  $[\text{Fe}(\text{II})(\text{CN})_6]^{4-}$ . On the other hand, the spectra of  $\text{Np}^{\text{IV}}/\text{Fe}^{\text{II}}$  and  $\text{Pu}^{\text{IV}}/\text{Fe}^{\text{II}}$  exhibit a reverse ratio of B over C intensity that increases from Np to Pu. To better understand the significance of this behavior in terms of bonding properties,

quantum chemical calculations have been undertaken, first on the hexacyanoferrate anions, then on the actinide hexacyanometallates. This work is currently under progress.

#### 4. Conclusion

Although the hexacyanoferrate family has been the subject of considerable interest in physical chemistry of the transition metal elements, very little is known about their actinide derivatives. Bridging cyanide ligands are indeed very good candidates to foster electronic delocalization and therefore to understand how the actinide elements may participate in electronic delocalization. Answering these questions related to both electronic and structural properties of actinide elements should cast light on some fundamental aspects of actinide chemistry and, technologically, in the development of specific ligands for selective ionic recognition.

To address this question we have launched a systematic study of the actinide hexacyanometallates by varying both atomic number (i.e. 5f orbital filling) and oxidation state. We have presented here our preliminary results on four compounds  $\text{Th}^{\text{IV}}/\text{Fe}^{\text{II}}$ ,  $\text{Np}^{\text{IV}}/\text{Fe}^{\text{II}}$ ,  $\text{Am}^{\text{III}}/\text{Fe}^{\text{II}}$  and  $\text{Cf}^{\text{III}}/\text{Fe}^{\text{II}}$ . Our strategy for both electronic and structural characterization is to probe the three components of the structure using X ray Absorption Spectroscopy : actinide, cyano ligand and iron. In the near future, coupling these data with theoretical calculation will provide a useful tool to simulate the absorption edges and therefore electronic effects.

#### Acknowledgement

Support for this research was provided by the Groupement National de Recherche PARIS, France, CEA/DEN/DSOE/RB and the European ACTINET network. XAS measurements were carried out at ESRF, a European user facility, at SSRL, a national user facility operated by Stanford University on behalf of the U.S. Department of Energy, Office of Basic Energy Sciences and at the ALS supported by the Office of Science, Office of Basic Energy Sciences, of the U.S. Department of Energy.

- 
- [1] Herren F P, Fischer A 1980 *Inorg. Chem.* **19** 956.
  - [2] Hocking R K, Wasinger E C, de Groot F, Hodgson K O, Hedman B, Solomon E I 2006 *J. Am. Chem. Soc.* **128** 10442.
  - [3] Cartier dit Moulin C, Champion G, Cafun J-D, Arrio M A, Bleuzen A 2007 *Angew. Chem. Int. Ed.* **46**, 1287.
  - [4] Kulyako Y M, Trofimov T I, Malikov D A, Lebedev I A, Myasoedov B F 1993 *Radiochem.* **35**, 549.
  - [5] Seaborg G T, Katz. J J *The Actinide Elements*. Mc Graw-Hill Book Compagny, Inc. New York, Toronto, London. 1954. vol. 14B, p 427.
  - [6] Krtil J 1967 *Radiochimica Acta* **7**, 30.
  - [7] Zhang L-P, Tanner P A, Mak T C 2006 *Eur. J. Inorg. Chem.* 1543.
  - [8] Xu X L, Hulliger F 1989 *J. Solid State Chem.* **80**, 120.
  - [9] Bonhoure I PhD thesis, *Structure moléculaire et électronique des hexacyanoferrates d'actinides*, Paris XI University, 2000 n°6290.
  - [10] Bonhoure I, Den Auwer C, Cartier dit Moulin C, Moisy P, Berthet J-C, Madic C 2000 *Can. J. Chem.* **78**, 1305.
  - [11] Dupouy G, Dumas T, Hennig C, Scheinost A, Conradson S, Den Auwer C manuscript in preparation.
  - [12] E. G. Fuster, R. Papalardo, E. Sanchez Marcos, D. Guillaumont, , C. Le Naour, E. Simoni, C. Hennig, A. Scheinost, C. Den Auwer, *Angew. Chem. Int. Ed.* Submitted.

- 
- [13] Ravel B, Newville M 2005 *J. Synchrotron Rad.* **12**, 537.
- [14] Rehr J J, Albers R C 2000 *Rev. Mod. Phys.* **72**, 621.
- [15] Mullica D F, Farmer J M, Cunningham B P, Kautz J A 2000 *J. Coord. Chem.* **49**, 239.
- [16] Mullica D F, Sappenfield E L 1989 *Powder Diffraction* **2**, 101.
- [17] Milligan W O 1982 *Inorg. Chim. Acta* **60**, 35.
- [18] D'Angelo P, De Panfilis S, Filipponi A, Persson I 2008 *Chem. Eur. J.* **14**, 3045.
- [19] Persson I, D'Angelo P, De Panfilis S, Sandström M, Eriksson L 2008 *Chem. Eur. J.* **14**, 3056.
- [20] Skanthakumar S, Antonio M R, Wilson R E, Soderholm L 2007 *Inorg. Chem.* **46**, 3485.
- [21] Lindqvist-Reis P, Apostolidis C, Rebizant J, Morgenstern A, Klenze R, Walter O, Fanghänel T, Haire R G 2007 *Angew. Chem. Int. Ed.* **46**, 919.
- [22] Revel R, Den Auwer C, Madic C, David F, Fourest B, Hubert S, Le Du J-F, Morss L R 1999 *Inorg. Chem.* **38**, 4139.
- [23] Allen P G, Bucher J J, Shuh D K, Edelstein N M, Craig I, 2000 *Inorg. Chem.* **39**, 595.
- [24] Hocking R K, Wasinger E C, de Groot F M, Hodgson K O, Hedman B, Solomon E I, 2006 *J. Am. Chem. Soc.* **128**, 10442.